



Deleterious *AHNAK2* Mutation as a Novel Biomarker for Immune Checkpoint Inhibitors in Non-Small Cell Lung Cancer

Yanan Cui^{1†}, Xinyin Liu^{1†}, Yuemin Wu^{1†}, Xiao Liang¹, Jiali Dai¹, Zhihong Zhang^{2*} and Renhua Guo^{1*}

¹ Department of Oncology, The First Affiliated Hospital of Nanjing Medical University, Nanjing, China, ² Department of Pathology, The First Affiliated Hospital of Nanjing Medical University, Nanjing, China

OPEN ACCESS

Edited by:

Nicolas Poté,
Bichat Hospital, France

Reviewed by:

Rohimah Mohamad,
Universiti Sains Malaysia (USM),
Malaysia
Edouard Guenzi,
Assistance Publique Hopitaux De
Paris, France

*Correspondence:

Renhua Guo
rghuo@njmu.edu.cn
Zhihong Zhang
zhangzh@njmu.edu.cn

[†]These authors have contributed
equally to this work

Specialty section:

This article was submitted to
Thoracic Oncology,
a section of the journal
Frontiers in Oncology

Received: 21 October 2021

Accepted: 14 February 2022

Published: 10 March 2022

Citation:

Cui Y, Liu X, Wu Y, Liang X, Dai J,
Zhang Z and Guo R (2022)
Deleterious *AHNAK2* Mutation
as a Novel Biomarker for Immune
Checkpoint Inhibitors in
Non-Small Cell Lung Cancer.
Front. Oncol. 12:798401.
doi: 10.3389/fonc.2022.798401

Immune checkpoint inhibitors (ICIs) have exhibited promising efficacy in non-small cell lung cancer (NSCLC), but the response occurs in only a minority of patients. In clinic, biomarkers such as TMB (tumor mutation burden) and PD-L1 (programmed cell death 1 ligand 1) still have their limitations in predicting the prognosis of ICI treatment. Hence, reliable predictive markers for ICIs are urgently needed. A public immunotherapy dataset with clinical information and mutational data of 75 NSCLC patients was obtained from cBioPortal as the discovery cohort, and another immunotherapy dataset of 249 patients across multiple cancer types was collected as the validation. Integrated bioinformatics analysis was performed to explore the potential mechanism, and immunohistochemistry studies were used to verify it. *AHNAK* nucleoprotein 2 (*AHNAK2*) was reported to have pro-tumor growth effects across multiple cancers, while its role in tumor immunity was unclear. We found that approximately 11% of the NSCLC patients harbored *AHNAK2* mutations, which were associated with promising outcomes to ICI treatments (ORR, $p = 0.013$). We further found that *AHNAK2* deleterious mutation (del-*AHNAK2*^{mut}) possessed better predictive function in NSCLC than non-deleterious *AHNAK2* mutation (PFS, OS, log-rank $p < 0.05$), potentially associated with stronger tumor immunogenicity and an activated immune microenvironment. This work identified del-*AHNAK2*^{mut} as a novel biomarker to predict favorable ICI response in NSCLC.

Keywords: NSCLC, *AHNAK2*, immune checkpoint inhibitors, biomarker, immune microenvironment

INTRODUCTION

Lung cancer, histologically differentiated into small cell lung cancer and non-small cell lung cancer, ranks among the most common cause of cancer-related death worldwide. Non-small cell lung cancer (NSCLC) accounts for about 85% of total cases routinely being treated with surgery, chemotherapy, radiation therapy, or targeted therapy. Nowadays, tumor immune checkpoint inhibitors (ICIs), including programmed death receptor 1 (PD-1), PD-ligand 1 (PD-L1), and cytotoxic T-lymphocyte-associated protein 4 (CTLA-4), have revolutionized NSCLC treatment (1, 2).

While ICIs have the potential for a durable response, the response occurs in only a minority of patients (3, 4). Therefore, predictive biomarkers of ICI treatment response are required to provide effective therapy. Although tumor mutation burden (TMB), PD-L1 expression, tumor immune microenvironment (TIME), and some specific gene mutations have been reported to be associated with ICI response (5–9), only a few of them have been validated in the clinic and even those validated biomarkers still had their limitations.

AHNAK2, a protein consisting of many extremely conserved duplicated fragments, shares extensive homology with *AHNAK1* and can interact with the C-terminal peptides of a variety of channel proteins (10). *AHNAK1* and *AHNAK2* co-localized with vinculin, suggesting that the proteins are components of the costameric network (11). It has previously been observed that *AHNAK2* is overexpressed in many cancers and acts as a poor prognostic biomarker in clear cell renal cell carcinoma (ccRCC), pancreatic ductal carcinoma (PDAC), papillary thyroid carcinoma (PTC), and lung adenocarcinoma (LUAD) (12–14). Several studies showed that *AHNAK2* promotes cell proliferation, migration, invasion, and epithelial–mesenchymal transition in LUAD *via* the MAPK pathway and the TGF- β /Smad3 pathway (15, 16). A recent study has demonstrated that the expression of *AHNAK2* is related to TIICs (tumor-infiltrating immune cells) (17). However, there is no study illustrating the relationship between *AHNAK2* and immune response.

In this study, we performed an extensive analysis of *AHNAK2* mutation using the previously published immunotherapy cohorts and aimed to explore the predictive value of the *AHNAK2* to ICI response in NSCLC patients.

MATERIALS AND METHODS

Data Download and Processing

The flow diagram of this study is depicted in **Figure 1**. To evaluate the predictive functions of *AHNAK2* in ICI-treated patients, we use the data accessed from the cBioPortal (<https://www.cbioportal.org>). A total of 75 NSCLC patients who received

anti-PD-L1 plus anti-cytotoxic T-cell lymphocyte-4 (anti-CTLA-4) treatment with whole-exome sequencing (WES) data (18) were included in our research as the discovery cohort. The validation cohort consisted of 249 patients across multiple cancer types who had received ICI therapy (19).

To study the mechanism underlying the association between *AHNAK2* mutation and ICI response, we obtained the WES data along with the corresponding mRNA expression data of 513 LUAD and 480 LUSC in TCGA cohort from the UCSC Xena data portal (<https://xenabrowser.net>). In addition, 305 Chinese NSCLC patients (20) from cBioPortal, referred to as Chinese cohort, were used to validate the findings.

Clinical Outcomes

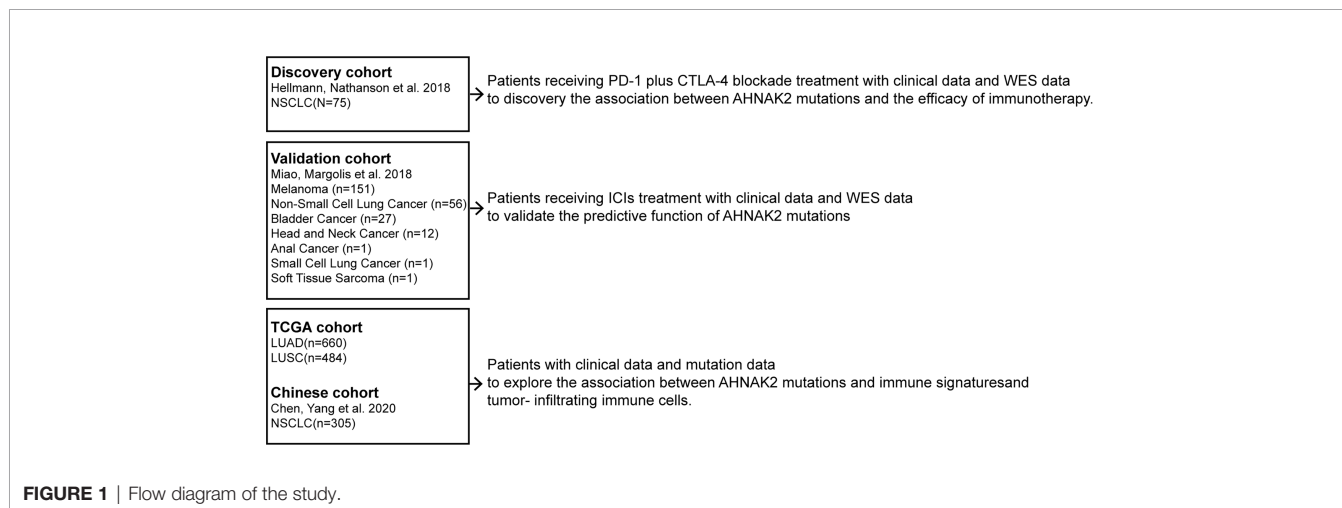
The primary clinical outcomes were objective response rate (ORR), progression-free survival (PFS), and overall survival (OS). ORR was assessed with Response Evaluation Criteria in Solid Tumors (RECIST) version 1.1. OS and PFS were measured from the start date of ICI therapy to the date of death or progression, respectively, in the ICI-treated cohort. Patients who had not died or progressed were censored at the date of their last scan. In TCGA cohort, OS and PFS were both assessed from the date of the first diagnosis.

PROVEAN Protein Database Evaluating the Mutational Impact on Protein Structure

Missense mutations might be deleterious or benign, on account of their effects on protein structure. The PROVEAN tool (<http://provean.jcvi.org>) was used to predict the function of missense variants (21). The cutoff for PROVEAN scores was set to -2.5 for high balanced accuracy, and we selected those amino acid changes with the PROVEAN score < -2.5 , indicating a deleterious effect on protein function.

Tumor Mutation Characteristics, Tumor Immunogenicity, and TIME Analysis

The cBioPortal online tool was used for visualization of the mutation rates of the top 20 genes and clinical characteristics. TMB was defined as the total number of non-synonymous



somatic, coding, base substitution, and indel mutations per megabase (Mb) of the genome examined (22). Neoantigen data in the TCGA cohort were obtained from Thorsson et al. (23).

GSEA was used to associate the gene signatures with *AHNAK2* deleterious mutation (del-*AHNAK2*^{mut}), *AHNAK2* non-deleterious mutation (non-del-*AHNAK2*^{mut}), and *AHNAK2* wild type (*AHNAK2*^{wt}). The normalized enrichment score (NES) is the primary statistic for examining gene set enrichment results. The single-sample gene set enrichment analysis (ssGSEA) method was applied to quantify the enrichment levels of the immune signatures in each sample using the “GSVA” R package (24). Twenty-nine characteristic immune signatures were obtained from a previous study (25).

The levels of TILs were calculated by analyzing the data from Saltz et al., who used deep learning-based lymphocyte classification to estimate the H&E-stained images from TCGA dataset (26). The infiltration statuses of twenty-two immune cells were analyzed using the CIBERSORT web portal (<https://cibersort.stanford.edu/>) (27).

Human Sample Collection and Immunohistochemistry

We collected five cases with two pulmonary nodules from the First Affiliated Hospital of Nanjing Medical University, both of which were confirmed as primary NSCLC by pathology. All samples were sequenced through whole-exome sequencing. Interestingly, in each case, one primary lung cancer was confirmed with *AHNAK2* mutation and the other was confirmed without *AHNAK2* mutation. Anti-CD3, anti-IFNG, and anti-GZMB immunohistochemistry (IHC) staining assays were performed on the tissue sections. The following antibodies were used: anti-CD3 (Servicebio, Wuhan, China, GB111337), anti-GZMB (Servicebio, GB14092), anti-IFNG (Abcam, Cambridge, CA, USA, ab231036). The digital quantitation of immunohistochemistry staining was conducted with HALO image analysis software (Indica Labs, Albuquerque, NM, USA).

Statistical Analyses

All analyses and statistical tests were carried out with the R software (version 3.6.1). Univariate Kaplan–Meier survival analysis was performed, and the survival curves were compared using the log-rank test. Fisher’s exact test was used to assess the enrichment of *AHNAK2* status with response (ORR). All comparisons were conducted using the Wilcoxon test. Statistical significance was set as 2-sided $p < 0.05$ for all comparisons.

RESULTS

Association Between *AHNAK2* Mutation and Better Clinical Benefit to ICIs in the Discovery Cohort

We collected 75 NSCLC patients who received ICI treatment with WES data as the discovery cohort. The genomic mutational landscape from the discovery cohort is displayed in **Figure 2A**

(including genes as suggested by NCCN guidelines and other oncogenes which had been reported to affect the efficacy of immunotherapies (28–31)). In agreement with previous studies, higher mutational rates of *TP53*, *KRAS*, and MMR-related genes were shown in responders relative to non-responders. On top of that, *AHNAK2* mutation was also observed to be enriched in responders (**Figure 2B**). The frequency of *AHNAK2* mutation was up to 11%, indicating that it was not a rare mutation in NSCLC. We found that the mutation of *AHNAK2* was statistically significantly associated with higher ORR (**Figure 2C**), suggesting that *AHNAK2* mutation might predict an improved clinical outcome for NSCLC patients treated with ICIs.

Interestingly, we found that all patients with *AHNAK2* mutation harbored *TP53* mutation in the discovery cohort. As *TP53* mutations are known to be correlated with response to immunotherapy, we compared ICI response between patients with *TP53* mutation only and patients with both *TP53* and *AHNAK2* mutation. As shown in **Figure 2D**, patients with *AHNAK2* and *TP53* co-mutations achieved a higher ORR than patients with *TP53* mutation only. Besides, among patients without *AHNAK2* mutation, *TP53* was not a statistically significant predictor. These results implied that clinical benefits of ICIs were even more remarkable in patients with *AHNAK2* mutation than in those with *TP53* mutation.

In addition, we compared the predictive value of *AHNAK2* mutation with other widely recognized ICI biomarkers. Here, we found that patients with high PD-L1 expression ($\geq 50\%$ percentage) had higher ORR than those with low PD-L1 expression ($< 50\%$ percentage), while this difference was not statistically significant (**Figure 2E**). Patients with high TMB level were more likely to benefit from the immunotherapy, which was also observed here (**Figure 2F**). Notably, *AHNAK2* mutation could identify patients with better response to immunotherapy among TMB-high patients (**Figure 2G**), indicating that the combination of *AHNAK2* mutation and TMB level could better stratify patients to identify those who are likely to benefit most from immunotherapy.

Del-*AHNAK2*^{mut} Is a Predictive, Not Prognostic, Biomarker of ICI Benefit

As illustrated in **Figure 3A**, most of the *AHNAK2* alterations were missense mutations, which can be partitioned into deleterious or benign, depending on whether they affect protein structures or not. To exclude the benign mutations that generally do not affect the protein function, the PROVEAN tool was applied to distinguish the missense mutations of *AHNAK2* with a high probability of impact on protein structures with a low probability (abbreviated as *AHNAK2*^{mis-high} and *AHNAK2*^{mis-low}, respectively). Since both truncating and mis-high mutations affect the biological function of the involved genes, we therefore grouped these two kinds of alterations as del-*AHNAK2*^{mut}. Relatively, patients with mis-low mutations of *AHNAK2* were defined as non-del-*AHNAK2*^{mut} whereas the patients without any *AHNAK2* mutations were categorized as the control group (*AHNAK2*^{wt}). A schematic of the workflow is shown in **Figure 3B**. As shown in

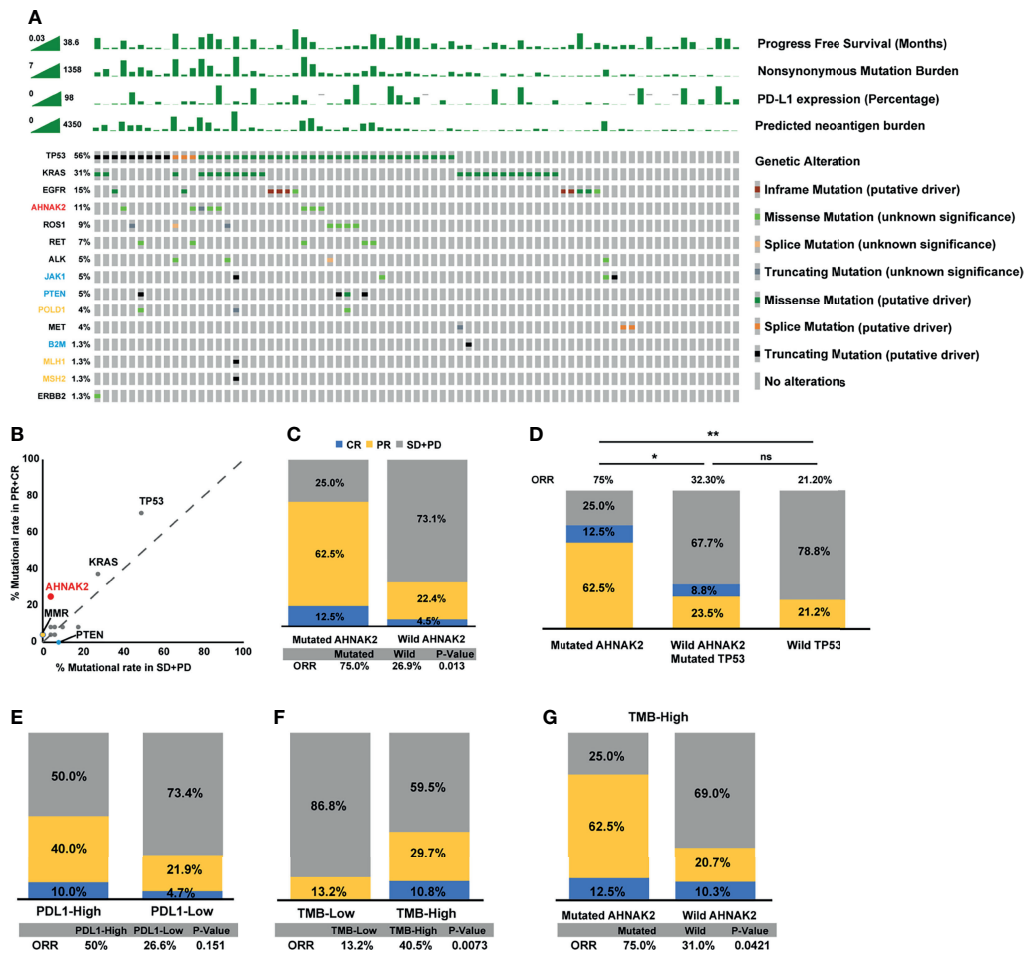


FIGURE 2 | *AHNAK2* mutations are significantly associated with better clinical benefit to ICIs in the discovery cohort. **(A)** Stacked plots show mutational burden, PD-L1 expression, and predicted neoantigen burden (histogram, top); mutations in TP53, KRAS, EGFR, ROS1, RET, ALK, MET, ERBB2 (genes recommended to be tested according to NCCN guidelines), and JAK1, PTEN, POLD1, B2M, MLH1, MSH2 (genes had been reported to affect the efficacy of immunotherapies; yellow represents positive predictors of immunotherapy, while blue represents negative predictors of immunotherapy) (tile plot, middle) and mutational marks (right). **(B)** Scatter diagram displays the mutational rate in patients having achieved objective response or progressive disease. MMR: mismatch repair genes (MLH1, MSH2). **(C)** Histogram depicting proportions of ORR in mutated *AHNAK2* and wild *AHNAK2* patients. **(D)** Histogram depicting proportions of ORR in mutated *AHNAK2*, mutated *TP53*/wild *AHNAK2*, and wild *TP53* patients. **(E)** Histogram depicting proportions of ORR in PDL1-High and PDL1-Low patients. **(F)** Histogram depicting proportions of ORR in mutated TMB-High and TMB-Low patients. **(G)** Histogram depicting proportions of ORR in mutated *AHNAK2* and wild *AHNAK2* among TMB-High patients (Mann-Whitney U test; ns, not significant; * $p < 0.05$, ** $p < 0.01$).

Figure 3C, the patients harboring deleterious *AHNAK2* mutations, not non-deleterious *AHNAK2* mutations, possessed a trend of better PFS than the patients with *AHNAK2*^{wt} in the discovery cohort.

To further assess the predictive value of deleterious *AHNAK2* mutations, we explored another pan-cancer immunotherapy cohort (19) as an independent external validation. In this validation cohort, the overall mutation frequency of *AHNAK2* was 14% with melanoma (17.2%) ranking the most prevalent cancer type followed by non-small cell lung cancer (12.5%) and bladder cancer (7.4%). Consistent with the results described above, the patients harboring deleterious *AHNAK2* mutation achieved better survival from ICI treatment compared with those without *AHNAK2* mutation (**Figures 3D, E**). Taking TCGA

cohort as a comparison, which includes the NSCLC patients without receiving immunotherapy, we found no significant survival differences between del-*AHNAK2*^{mut} and *AHNAK2*^{wt} (**Figures 3F, G**). These results suggested that del-*AHNAK2*^{mut} was not linked with prognosis but was associated with significant immunotherapeutic efficacy independently, which delineated the potential predictive value of del-*AHNAK2*^{mut} in immunotherapy against NSCLC.

Association Between *AHNAK2*^{mut} and Higher Tumor Immunogenicity

To investigate the potential mechanism by which *AHNAK2* mutations influence the sensitivity of ICI therapy, we first analyzed the mutational burden (TMB) and neoantigen load

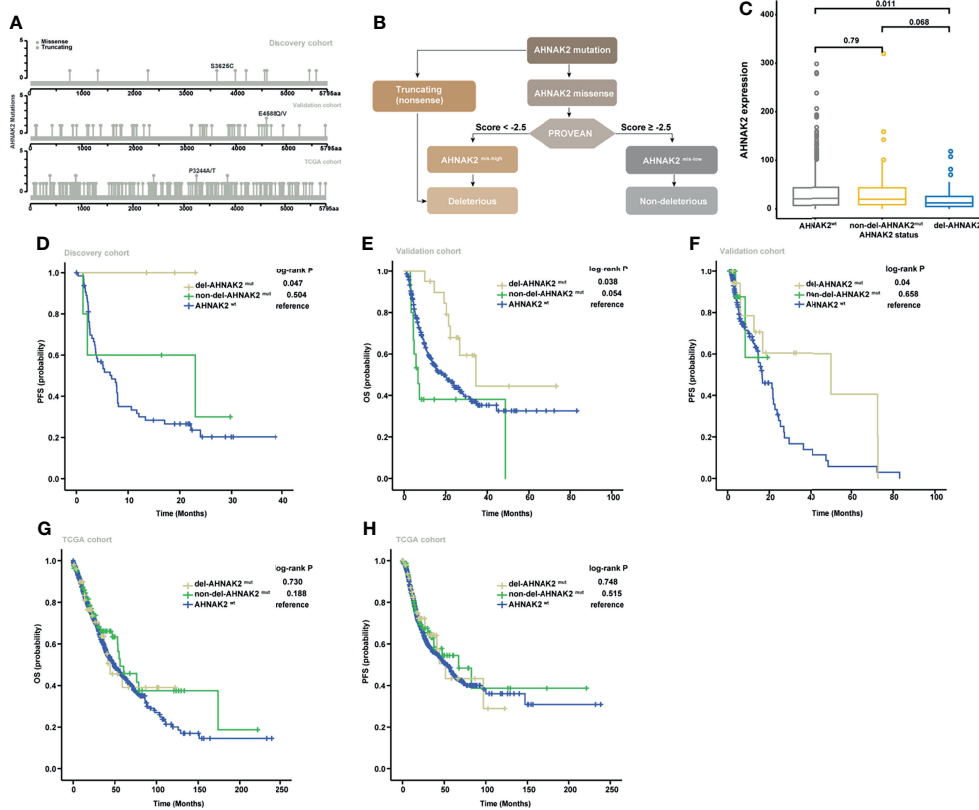


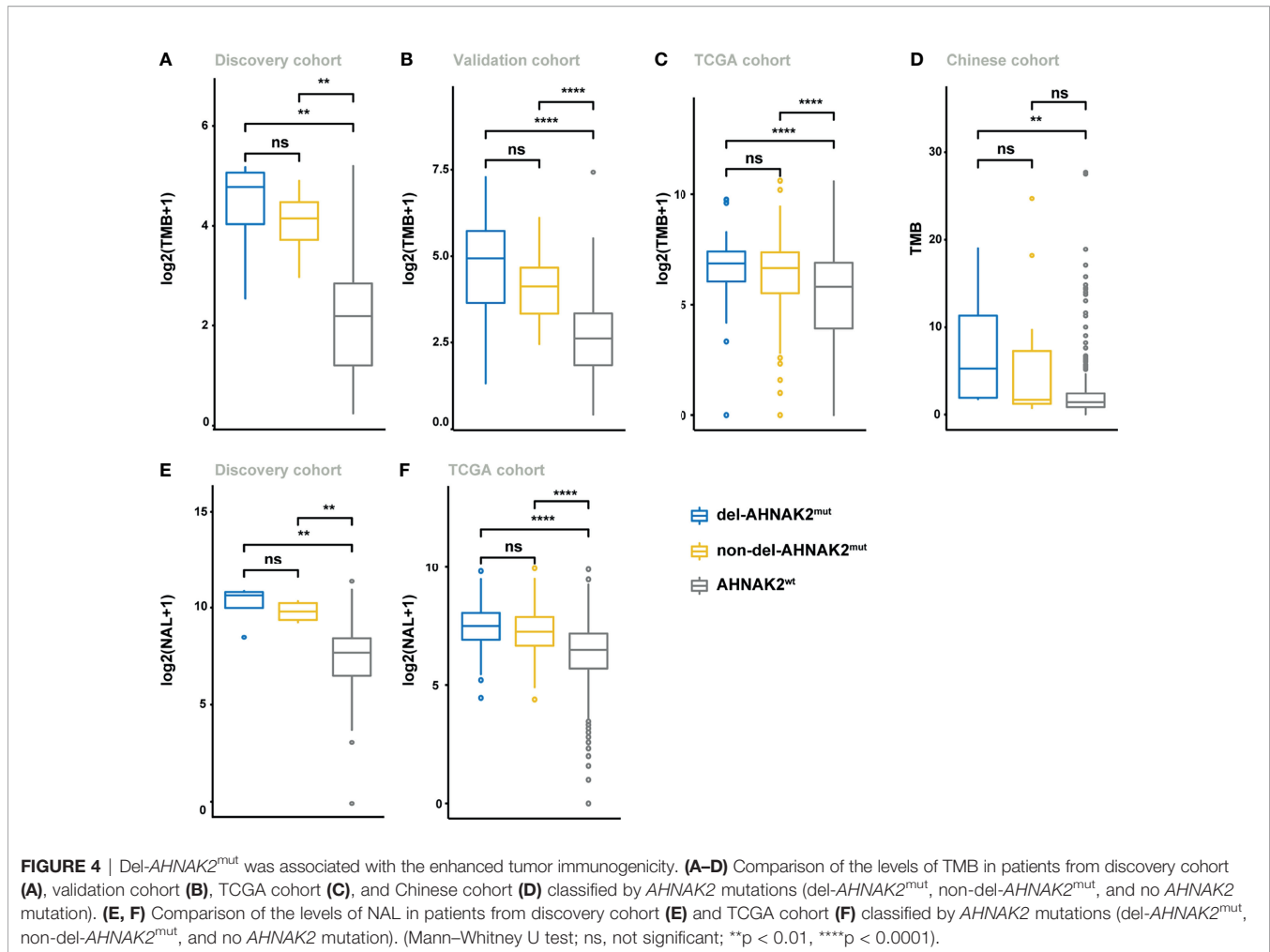
FIGURE 3 | Validation of the predictive significance of *AHNAK2* in pan-cancer. **(A)** Lollipop plots showing the locus distribution of mutations across the *AHNAK2*-altered patient cohorts. **(B)** Flow diagram of the identification of *del-AHNAK2*^{mut} and *non-del-AHNAK2*^{mut} by mutational forms and PROVEAN. **(C)** Kaplan-Meier curves of PFS in the discovery cohort classified by *AHNAK2* mutations. **(D)** Kaplan-Meier curves of OS in the validation cohort classified by *AHNAK2* mutations. **(E)** Kaplan-Meier curves of PFSS in the validation cohort classified by *AHNAK2* mutations. **(F)** Kaplan-Meier curves of OS in the TCGA cohort classified by *AHNAK2* mutations. **(G)** Kaplan-Meier curves of PFS in the TCGA cohort classified by *AHNAK2* mutations.

(NAL). As shown in **Figure 4A**, higher TMB levels were observed in *AHNAK2*^{mut} tumors in the discovery cohort, which was verified in the validation cohort, TCGA cohort, and Chinese cohort (**Figures 4B–D**). In addition, the level of NAL was significantly higher in the *AHNAK2*^{mut} tumors as well, relative to the *AHNAK2*^{wt} group (**Figures 4E, F**). These results suggested that *AHNAK2*^{mut} tumors were strongly related to enhanced tumor immunogenicity, firmly supporting its predictive value for ICI therapy.

Impact of *del-AHNAK2*^{mut} on Activated Immune Microenvironment

Despite the undifferentiated levels of TMB and NAL observed in the *del-AHNAK2*^{mut} and *non-del-AHNAK2*^{mut} groups, the potential mechanisms to immune activation might be dissimilar between these two groups. Cytotoxic T lymphocytes (CD8+ T cells and NK cells) were major mediators of the innate and adaptive antitumor immune response and can use cytotoxic granules containing perforin and granzymes to lyse cancer cells. GSEA revealed prominent enrichment of signatures related to

CD8+ T cell and NK cell activation in the *del-AHNAK2*^{mut} group, compared with the *non-del-AHNAK2*^{mut} and *AHNAK2*^{wt} groups (**Figures 5A, B**). In addition, enhanced IFN- γ signaling was also observed in the *del-AHNAK2*^{mut} group (**Figure 5C**). Previous studies have implicated that the efficiency of anti-PD-L1 and anti-CTLA-4 therapy was dependent on IFN- γ . Produced by cytotoxic immune cells, IFN- γ could facilitate CD8+ T cell and NK cell infiltration (32). Next, to test whether *del-AHNAK2*^{mut} was associated with cytotoxic T lymphocyte function and infiltration, the ssGSEA method was utilized to evaluate the immune status of each patient by analyzing the expression profiles of 29 immune signatures (25). As expected, we found that *del-AHNAK2*^{mut} tumors expressed higher cytolytic activity scores (**Figure 5D**), indicating that *del-AHNAK2*^{mut} might liberate CTL cell effector functions. Beyond this, the *del-AHNAK2*^{mut} tumors were also characterized by more CD8+ T cell and NK cell infiltrations according to the ssGSEA results (**Figure 5E**). To cross-examine the above results with different methods of evaluating immune cells, we analyzed the distribution of 22 immune cells based on the CIBERSORT



method, observing an increase of CD8+ T cells and NK cells in the tumors with del-AHNAK2^{mut}, relative to those with non-del-AHNAK2^{mut} and AHNAK2^{wt} (Figure 5F). According to the TIL fraction data estimated from hematoxylin and eosin-stained (H&E-stained) slides (26), we found that the TIL fraction of the del-AHNAK2^{mut} tumors was higher than that of the AHNAK2^{wt} tumors (Figure 5G). To further validate the above results, we also analyzed the RNA-sequencing data from the Chinese cohort and obtained similar findings for the high T cell and NK cell infiltration in del-AHNAK2^{mut} tumor (Figure 5H).

Immunohistochemistry Confirmed the Association Between del-AHANK2^{mut} and Activated Immune Microenvironment

We collected 5 patients with multiple lung cancer (MPLC) from the First Affiliated Hospital of Nanjing Medical University, and each patient owned two primary tumors (Figure 6A). After surgical treatment, a total of 10 resected tumors from the 5 patients were processed for whole-exome sequencing. Many studies have revealed that in the context of identical constitutional genetic background and environmental exposure, different lung cancers

in the same individual have distinct genomic profiles and can be driven by distinct molecular events (33, 34). In our study, few shared mutations were detected between two tumors from the same patient by performing whole-exome sequencing (Figures S1A, B). Interestingly, in each patient from our study, one tumor was conformed with deleterious AHNAK2 mutation and the other was conformed without AHNAK2 mutation (Figure S1A). In this unique model, tumors with different mutation statuses of AHNAK2 came from the same patient, so some interference caused by genetic background and lifestyle among patients can be reduced to a large extent, enabling us to better explore the association between del-AHNAK2^{mut} and the immune environment. As shown in Figure 6B, immunohistochemical (IHC) staining of CD3 confirmed the presence of tumor-infiltrating T cells in the del-AHNAK2^{mut} tumors. In addition, CD3, IFNG, and GZMB were markedly increased in del-AHNAK2^{mut} tumors compared to AHNAK2^{wt} tumors (Figures 6C, D).

To sum up, del-AHNAK2^{mut} positively correlated with activated CTL effector functions, IFN- γ signaling, and infiltration of TILs, which contributed to the activated immune microenvironment.

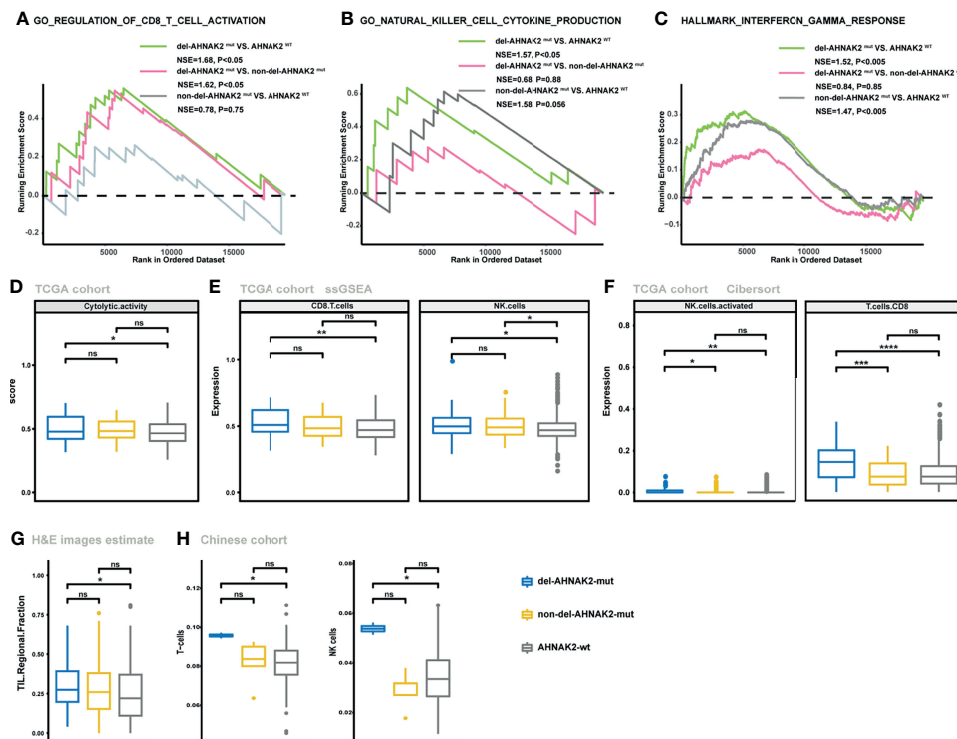


FIGURE 5 | The mutation status of *AHNAK2* was associated with the activated immune microenvironment. **(A–C)** GSEA of signatures related to CD8 T cell activation **(A)**, NK cell activation **(B)**, and IFN- γ **(C)** in comparisons between NSCLC samples with del-*AHNAK2*^{mut}, non-del-*AHNAK2*^{mut}, and no *AHNAK2* mutation. **(D)** Comparison of the cytolytic activity score between *AHNAK2*^{wt}, del-*AHNAK2*^{mut}, and non-del-*AHNAK2*^{mut} tumors by the ssGSEA method based on TCGA RNA-sequencing data. **(E)** Comparison of the infiltration degree of immune cells by the ssGSEA method based on RNA-sequencing data between *AHNAK2*^{wt}, del-*AHNAK2*^{mut}, and non-del-*AHNAK2*^{mut} tumors. **(F)** Comparison of the infiltration degree of immune cells by the CIBERSORT analysis. **(G)** Comparison of the TIL regional fractions based on estimates from processing diagnostic H&E images between *AHNAK2*^{wt}, del-*AHNAK2*^{mut}, and non-del-*AHNAK2*^{mut} tumors. **(H)** Comparison of the infiltration degree of immune cells in the Chinese NSCLC cohort. (Mann–Whitney U test; ns, not significant; *p < 0.05, **p < 0.01, ***p < 0.001, ****p < 0.0001)

DISCUSSION

In recent years, immunotherapy has become a critical milestone of oncology. The growing types of immunotherapy treatments are put into clinical application. Meanwhile, the selection of patients who could get benefit from immunotherapy has also become a formidable clinical problem. Given that the PD-L1 expression or TMB level could not be sufficient to select patients who may benefit the most from immunotherapy, many studies dedicated to identify more precise biomarkers to predict the efficacy of immunotherapy and genetic alterations are among the best-studied (35). For example, gene mutation biomarkers such as *POLE*, *ARID1*, and *FGFR4* increase the TMB level, expression of PD-L1, and activation of the cellular immunity CD8+ tumor infiltration level (36–38). However, these results were not imperfect.

AHNAK1 and *AHNAK2* are two members of the *AHNAK* family (10), and several studies have strived to decode their function. *AHNAK* can serve as a structural scaffold to mediate the assembly of multiprotein complexes. Meanwhile, significant

evidence has been provided to characterize the role of *AHNAK* in membrane repair and calcium channel regulation (39, 40). In recent studies, *AHNAK1* has also been proved as a tumor suppressor in several cancers, including colorectal cancer, gastric cancer, breast cancer, glioma, and lung cancer (41–45). However, as a homologous gene, *AHNAK2* appears to play the opposite function promoting cell proliferation, migration, invasion, and epithelial–mesenchymal transition. *AHNAK2* expression negatively correlated with activated CD8+ T cell infiltration. We thus posit that the dysfunction of *AHNAK2* may contribute to tumor immunity and improved outcomes in ICI-treated NSCLC.

To the best of our knowledge, this is the first report to propose the predictive value of the *AHNAK2* in ICI treatment. In our study, we demonstrated that patients harboring *AHNAK2* mutations were likely to have a better response to ICI treatment. Importantly, among all kinds of *AHNAK2* alterations, compared to non-deleterious, deleterious mutation might exhibit more predictive power. Del-*AHNAK2*^{mut} was closely correlated with the higher TMB and NAL level and

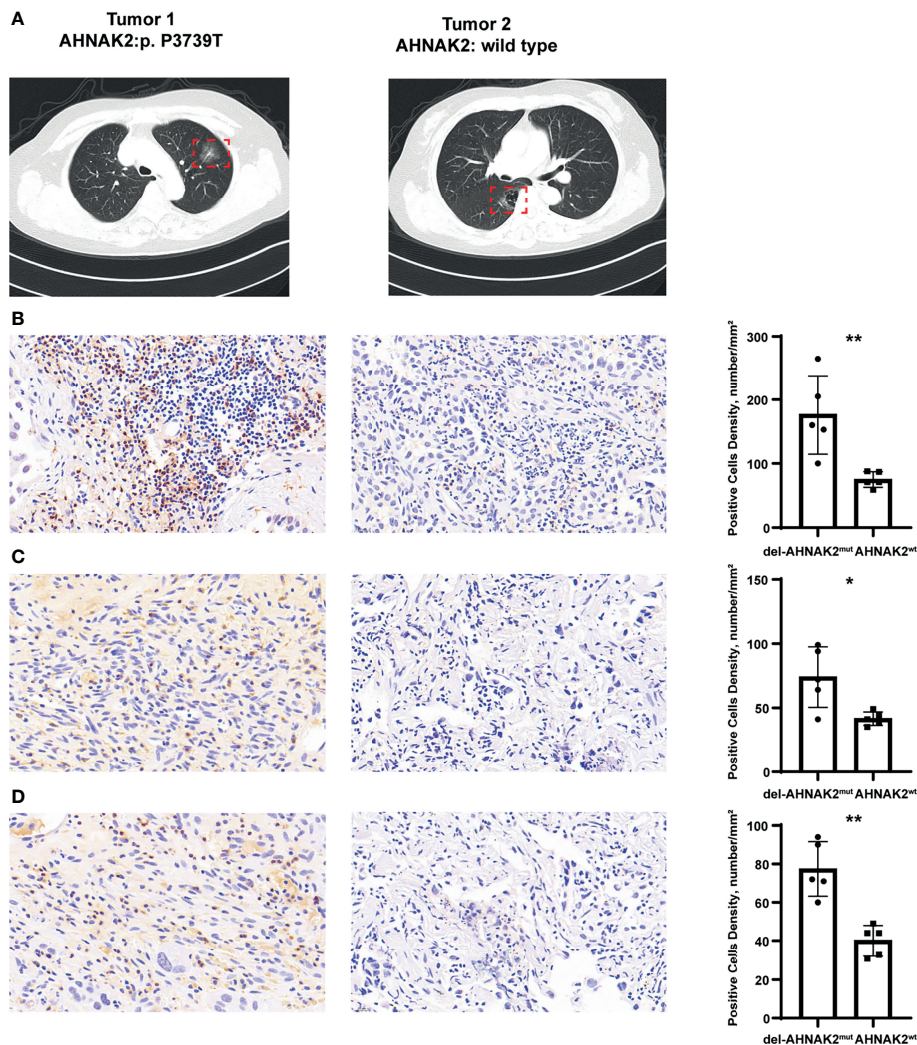


FIGURE 6 | Immunohistochemical staining to evaluate the association between del-*AHNAK2*^{mut} and activated immune microenvironment. **(A)** Computed tomography (CT) imaging of the representative MPLC patient. **(B–D)** Quantitative immunohistochemistry (IHC) analysis of CD3 **(B)**, GZMB **(C)**, and IFNG **(D)** protein expression in the del-*AHNAK2*^{mut} and *AHNAK2*^{wt} groups (n = 5/group). Representative micrographs of these samples are shown. Data represent the mean ± SD. (Mann–Whitney U test; *p < 0.05, **p < 0.01).

activation of the NK cells, T cells, and IFN- γ signaling, which in turn initiate a therapeutic immune response in NSCLC.

A major limitation of the study is the limited sample size. *AHNAK2* mutation was not included in the routine gene panel; it could only be detected with whole exon sequencing. So far, only two public immunotherapy studies have used the whole exon sequencing, which has been included in our study as the discovery cohort and validation cohort. To compensate for this limitation, RNA-seq data from the TCGA cohort and Chinese cohort were used to verify the association between del-*AHNAK2*^{mut} and activated immune microenvironment. Further studies are needed to decrypt the effect of *AHNAK2* in cancer immunotherapy. In addition, while our results suggest that del-*AHNAK2*^{mut} may play a role in the regulation of the

tumor microenvironment, no specific molecular mechanisms were determined. An earlier report raised a potential mechanism by which *AHNAK1* affects CTL function by disrupting calcium entry formation (46). In our study, we also found that *AHNAK2* loss-of-function mutation could liberate CTL (CD8+ T cells and NK cells) effector function. As the homolog gene of *AHNAK1*, whether *AHNAK2* can also influence the calcium entry which in turn regulates TIILs remains a subject for future research.

In conclusion, we proposed that del-*AHNAK2*^{mut} could serve as a novel biomarker for NSCLC patients with ICI treatment. Predictive biomarkers to ICIs, such as the TMB level, NAL level, and TIICs, are closely associated with deleterious *AHNAK2* mutations.

DATA AVAILABILITY STATEMENT

The original contributions presented in the study are included in the article/**Supplementary Material**. Further inquiries can be directed to the corresponding authors.

ETHICS STATEMENT

Written informed consent was obtained from the individual(s) for the publication of any potentially identifiable images or data included in this article.

AUTHOR CONTRIBUTIONS

YC: conceptualization, methodology, software, data curation, writing—original draft preparation. XyL: writing—reviewing and

REFERENCES

- Borghaei H, Paz-Ares L, Horn L, Spigel DR, Steins M, Ready NE, et al. Nivolumab Versus Docetaxel in Advanced Nonsquamous Non-Small-Cell Lung Cancer. *N Engl J Med* (2015) 373(17):1627–39. doi: 10.1056/NEJMoa1507643
- Reck M, Rodríguez-Abreu D, Robinson AG, Hui R, Csósz T, Fülöp A, et al. Pembrolizumab Versus Chemotherapy for PD-L1-Positive Non-Small-Cell Lung Cancer. *N Engl J Med* (2016) 375(19):1823–33. doi: 10.1056/NEJMoa1606774
- Rotte A, Jin JY, Lemaire V. Mechanistic Overview of Immune Checkpoints to Support the Rational Design of Their Combinations in Cancer Immunotherapy. *Ann Oncol: Off J Eur Soc Med Oncol* (2018) 29(1):71–83. doi: 10.1093/annonc/mdx686
- Ramos-Casals M, Brahmer JR, Callahan MK, Flores-Chávez A, Keegan N, Khamashta MA, et al. Immune-Related Adverse Events of Checkpoint Inhibitors. *Nat Rev Dis Primers* (2020) 6(1):38. doi: 10.1038/s41572-020-0160-6
- Wu HX, Chen YX, Wang ZX, Zhao Q, He MM, Wang YN, et al. Alteration in TET1 as Potential Biomarker for Immune Checkpoint Blockade in Multiple Cancers. *J Immunother Cancer* (2019) 7(1):264. doi: 10.1186/s40425-019-0737-3
- Hakimi AA, Voss MH, Kuo F, Sanchez A, Liu M, Nixon BG, et al. Transcriptomic Profiling of the Tumor Microenvironment Reveals Distinct Subgroups of Clear Cell Renal Cell Cancer: Data From a Randomized Phase III Trial. *Cancer Discovery* (2019) 9(4):510–25. doi: 10.1158/2159-8290.CD-18-0957
- Ready N, Hellmann MD, Awad MM, Otterson GA, Gutierrez M, Gainor JF, et al. First-Line Nivolumab Plus Ipilimumab in Advanced Non-Small-Cell Lung Cancer (CheckMate 568): Outcomes by Programmed Death Ligand 1 and Tumor Mutational Burden as Biomarkers. *J Clin Oncol: Off J Am Soc Clin Oncol* (2019) 37(12):992–1000. doi: 10.1200/JCO.18.01042
- Zhou H, Liu J, Zhang Y, Huang Y, Shen J, Yang Y, et al. PBRM1 Mutation and Preliminary Response to Immune Checkpoint Blockade Treatment in Non-Small Cell Lung Cancer. *NPJ Precis Oncol* (2020) 4:6. doi: 10.1038/s41698-020-0112-3
- Ott PA, Bang YJ, Piha-Paul SA, Razak ARA, Bennouna J, Soria JC, et al. T-Cell-Inflamed Gene-Expression Profile, Programmed Death Ligand 1 Expression, and Tumor Mutational Burden Predict Efficacy in Patients Treated With Pembrolizumab Across 20 Cancers: KEYNOTE-028. *J Clin Oncol* (2019) 37(4):318–27. doi: 10.1200/JCO.2018.78.2276
- Komuro A, Masuda Y, Kobayashi K, Babbitt R, Gunel M, Flavell RA, et al. The AHNAKs are a Class of Giant Propeller-Like Proteins That Associate With

editing. YW: data curation. XL: methodology. JD: data curation. ZZ and RG: supervision, project administration. All authors contributed to the article and approved the submitted version.

FUNDING

This work was supported by grants from the National Natural Science Foundation of China (81972188) and the Medical Important Talents of Jiangsu Province (ZDRCA2016024).

SUPPLEMENTARY MATERIAL

The Supplementary Material for this article can be found online at: <https://www.frontiersin.org/articles/10.3389/fonc.2022.798401/full#supplementary-material>

- Calcium Channel Proteins of Cardiomyocytes and Other Cells. *Proc Natl Acad Sci USA* (2004) 101(12):4053–8. doi: 10.1073/pnas.0308619101
- Marg A, Haase H, Neumann T, Kouno M, Morano I. AHNAK1 and AHNAK2 Are Costameric Proteins: AHNAK1 Affects Transverse Skeletal Muscle Fiber Stiffness. *Biochem Biophys Res Commun* (2010) 401(1):143–8. doi: 10.1016/j.bbrc.2010.09.030
- Wang M, Li X, Zhang J, Yang Q, Chen W, Jin W, et al. AHNAK2 Is a Novel Prognostic Marker and Oncogenic Protein for Clear Cell Renal Cell Carcinoma. *Theranostics* (2017) 7(5):1100–13. doi: 10.7150/tno.18198
- Xie Z, Lun Y, Li X, He Y, Wu S, Wang S, et al. Bioinformatics Analysis of the Clinical Value and Potential Mechanisms of AHNAK2 in Papillary Thyroid Carcinoma. *Aging* (2020) 12(18):18163–80. doi: 10.18632/aging.103645
- Lu D, Wang J, Shi X, Yue B, Hao J. AHNAK2 Is a Potential Prognostic Biomarker in Patients With PDAC. *Oncotarget* (2017) 8(19):31775–84. doi: 10.18632/oncotarget.15990
- Liu G, Guo Z, Zhang Q, Liu Z, Zhu D. AHNAK2 Promotes Migration, Invasion, and Epithelial-Mesenchymal Transition in Lung Adenocarcinoma Cells via the TGF- β /Smad3 Pathway. *Oncotargets Ther* (2020) 13:12893–903. doi: 10.2147/OTT.S281517
- Wang D-W, Zheng H-Z, Cha N, Zhang X-J, Zheng M, Chen M-M, et al. Down-Regulation of AHNAK2 Inhibits Cell Proliferation, Migration and Invasion Through Inactivating the MAPK Pathway in Lung Adenocarcinoma. *Technol Cancer Res Treat* (2020) 19:1533033820957006. doi: 10.1177/1533033820957006
- Zheng M, Liu J, Bian T, Liu L, Sun H, Zhou H, et al. Correlation Between Prognostic Indicator AHNAK2 and Immune Infiltrates in Lung Adenocarcinoma. *Int Immunopharmacol* (2021) 90:107134. doi: 10.1016/j.intimp.2020.107134
- Hellmann MD, Nathanson T, Rizvi H, Creelan BC, Sanchez-Vega F, Ahuja A, et al. Genomic Features of Response to Combination Immunotherapy in Patients With Advanced Non-Small-Cell Lung Cancer. *Cancer Cell* (2018) 33(5):843–52.e4. doi: 10.1016/j.ccell.2018.04.005
- Miao D, Margolis CA, Vokes NI, Liu D, Taylor-Weiner A, Wankowicz SM, et al. Genomic Correlates of Response to Immune Checkpoint Blockade in Microsatellite-Stable Solid Tumors. *Nat Genet* (2018) 50(9):1271–81. doi: 10.1038/s41588-018-0200-2
- Chen J, Yang H, Teo ASM, Amer LB, Sherbaf FG, Tan CQ, et al. Genomic Landscape of Lung Adenocarcinoma in East Asians. *Nat Genet* (2020) 52(2):177–86. doi: 10.1038/s41588-019-0569-6
- Choi Y, Sims GE, Murphy S, Miller JR, Chan AP. Predicting the Functional Effect of Amino Acid Substitutions and Indels. *PLoS One* (2012) 7(10):e46688. doi: 10.1371/journal.pone.0046688
- Yarchoan M, Hopkins A, Jaffee EM. Tumor Mutational Burden and Response Rate to PD-1 Inhibition. *N Engl J Med* (2017) 377(25):2500–1. doi: 10.1056/NEJMc1713444

23. Thorsson V, Gibbs DL, Brown SD, Wolf D, Bortone DS, Ou Yang T-H, et al. The Immune Landscape of Cancer. *Immunity* (2018) 48(4):812–30.e14. doi: 10.1016/j.immuni.2018.03.02
24. Hänzelmann S, Castelo R, Guinney J. GSEA: Gene Set Variation Analysis for Microarray and RNA-Seq Data. *BMC Bioinf* (2013) 14:7. doi: 10.1186/1471-2105-14-7
25. He Y, Jiang Z, Chen C, Wang X. Classification of Triple-Negative Breast Cancers Based on Immunogenomic Profiling. *J Exp Clin Cancer Res: CR* (2018) 37(1):327. doi: 10.1186/s13046-018-1002-1
26. Saltz J, Gupta R, Hou L, Kurc T, Singh P, Nguyen V, et al. Spatial Organization and Molecular Correlation of Tumor-Infiltrating Lymphocytes Using Deep Learning on Pathology Images. *Cell Rep* (2018) 23(1):181–93.e7. doi: 10.1016/j.celrep.2018.03.086
27. Newman AM, Liu CL, Green MR, Gentles AJ, Feng W, Xu Y, et al. Robust Enumeration of Cell Subsets From Tissue Expression Profiles. *Nat Methods* (2015) 12(5):453–7. doi: 10.1038/nmeth.3337
28. Rizvi NA, Hellmann MD, Snyder A, Kvistborg P, Makarov V, Havel JJ, et al. Cancer Immunology. Mutational Landscape Determines Sensitivity to PD-1 Blockade in Non-Small Cell Lung Cancer. *Science* (2015) 348(6230):124–8. doi: 10.1126/science.aaa1348
29. Haradhvala NJ, Kim J, Maruvka YE, Polak P, Rosebrock D, Livitz D, et al. Distinct Mutational Signatures Characterize Concurrent Loss of Polymerase Proofreading and Mismatch Repair. *Nat Commun* (2018) 9(1):1746. doi: 10.1038/s41467-018-04002-4
30. Dong Z-Y, Zhong W-Z, Zhang X-C, Su J, Xie Z, Liu S-Y, et al. Potential Predictive Value of and Mutation Status for Response to PD-1 Blockade Immunotherapy in Lung Adenocarcinoma. *Clin Cancer Res: Off J Am Assoc Cancer Res* (2017) 23(12):3012–24. doi: 10.1158/1078-0432.CCR-16-2554
31. Miao D, Margolis CA, Gao W, Voss MH, Li W, Martini DJ, et al. Genomic Correlates of Response to Immune Checkpoint Therapies in Clear Cell Renal Cell Carcinoma. *Science* (2018) 359(6377):801–6. doi: 10.1126/science.aan5951
32. Jorgovanovic D, Song M, Wang L, Zhang Y. Roles of IFN- γ in Tumor Progression and Regression: A Review. *biomark Res* (2020) 8:49. doi: 10.1186/s40364-020-00228-x
33. Ma P, Fu Y, Cai M-C, Yan Y, Jing Y, Zhang S, et al. Simultaneous Evolutionary Expansion and Constraint of Genomic Heterogeneity in Multifocal Lung Cancer. *Nat Commun* (2017) 8(1):823. doi: 10.1038/s41467-017-00963-0
34. Liu Y, Zhang J, Li L, Yin G, Zhang J, Zheng S, et al. Genomic Heterogeneity of Multiple Synchronous Lung Cancer. *Nat Commun* (2016) 7:13200. doi: 10.1038/ncomms13200
35. Rossi G, Russo A, Tagliamento M, Tuzi A, Nigro O, Vallome G, et al. Precision Medicine for NSCLC in the Era of Immunotherapy: New Biomarkers to Select the Most Suitable Treatment or the Most Suitable Patient. *Cancers* (2020) 12(5):1125. doi: 10.3390/cancers12051125
36. Song Z, Cheng G, Xu C, Wang W, Shao Y, Zhang Y, et al. Clinicopathological Characteristics of POLE Mutation in Patients With Non-Small-Cell Lung Cancer. *Lung Cancer (Amsterdam Netherlands)* (2018) 118:57–61. doi: 10.1016/j.lungcan.2018.02.004
37. Wang L, Ren Z, Yu B, Tang J. Development of Nomogram Based on Immune-Related Gene FGFR4 for Advanced Non-Small Cell Lung Cancer Patients With Sensitivity to Immune Checkpoint Inhibitors. *J Trans Med* (2021) 19(1):22. doi: 10.1186/s12967-020-02679-0
38. Sun D, Tian L, Zhu Y, Wo Y, Liu Q, Liu S, et al. Subunits of ARID1 Serve as Novel Biomarkers for the Sensitivity to Immune Checkpoint Inhibitors and Prognosis of Advanced Non-Small Cell Lung Cancer. *Mol Med (Cambridge Mass.)* (2020) 26(1):78. doi: 10.1186/s10020-020-00208-9
39. Sussman J, Stokoe D, Ossina N, Shtivelman E. Protein Kinase B Phosphorylates AHNAK and Regulates Its Subcellular Localization. *J Cell Biol* (2001) 154(5):1019–30. doi: 10.1083/jcb.200105121
40. Davis TA, Loos B, Engelbrecht AM. AHNAK: The Giant Jack of All Trades. *Cell Signal* (2014) 26(12):2683–93. doi: 10.1016/j.cellsig.2014.08.017
41. Shen E, Wang X, Liu X, Lv M, Zhang L, Zhu G, et al. MicroRNA-93-5p Promotes Epithelial-Mesenchymal Transition in Gastric Cancer by Repressing Tumor Suppressor AHNAK Expression. *Cancer Cell Int* (2020) 20:76. doi: 10.1186/s12935-019-1092-7
42. Cho W-C, Jang J-E, Kim K-H, Yoo B-C, Ku J-L. SORBS1 Serves a Metastatic Role via Suppression of AHNAK in Colorectal Cancer Cell Lines. *Int J Oncol* (2020) 56(5):1140–51. doi: 10.3892/ijo.2020.5006
43. Zhao Z, Xiao S, Yuan X, Yuan J, Zhang C, Li H, et al. AHNAK as a Prognosis Factor Suppresses the Tumor Progression in Glioma. *J Cancer* (2017) 8(15):2924–32. doi: 10.7150/jca.20277
44. Chen B, Wang J, Dai D, Zhou Q, Guo X, Tian Z, et al. AHNAK Suppresses Tumour Proliferation and Invasion by Targeting Multiple Pathways in Triple-Negative Breast Cancer. *J Exp Clin Cancer Res: CR* (2017) 36(1):65. doi: 10.1186/s13046-017-0522-4
45. Park JW, Kim IY, Choi JW, Lim HJ, Shin JH, Kim YN, et al. AHNAK Loss in Mice Promotes Type II Pneumocyte Hyperplasia and Lung Tumor Development. *Mol Cancer Res: MCR* (2018) 16(8):1287–98. doi: 10.1158/1541-7786.MCR-17-0726
46. Matza D, Badou A, Jha MK, Willinger T, Antov A, Sanjabi S, et al. Requirement for AHNAK1-Mediated Calcium Signaling During T Lymphocyte Cytolysis. *Proc Natl Acad Sci USA* (2009) 106(24):9785–90. doi: 10.1073/pnas.0902844106

Conflict of Interest: The authors declare that the research was conducted in the absence of any commercial or financial relationships that could be construed as a potential conflict of interest.

Publisher's Note: All claims expressed in this article are solely those of the authors and do not necessarily represent those of their affiliated organizations, or those of the publisher, the editors and the reviewers. Any product that may be evaluated in this article, or claim that may be made by its manufacturer, is not guaranteed or endorsed by the publisher.

Copyright © 2022 Cui, Liu, Wu, Liang, Dai, Zhang and Guo. This is an open-access article distributed under the terms of the Creative Commons Attribution License (CC BY). The use, distribution or reproduction in other forums is permitted, provided the original author(s) and the copyright owner(s) are credited and that the original publication in this journal is cited, in accordance with accepted academic practice. No use, distribution or reproduction is permitted which does not comply with these terms.